

# Long-range ferromagnetism of Mn<sub>12</sub> acetate single-molecule magnets under a transverse magnetic field

F. Luis<sup>\*1</sup>, J. Campo<sup>1</sup>, J. Gómez<sup>2</sup>, G. J. McIntyre<sup>3</sup>, J. Luzón<sup>1</sup>, and D. Ruiz-Molina<sup>2</sup>  
<sup>1</sup>*Instituto de Ciencia de Materiales de Aragón, CSIC-Universidad de Zaragoza, 50009 Zaragoza, Spain.*  
<sup>2</sup>*Institut de Ciència de Materials de Barcelona, Campus de la UAB, Bellaterra 08193, Spain.*  
<sup>3</sup>*Institut Laue Langevin, 6 rue Jules Horowitz, 38042 Grenoble, France.*

We use neutron diffraction to probe the magnetization components of a crystal of Mn<sub>12</sub> single-molecule magnets. Each of these molecules behaves, at low temperatures, as a nanomagnet with spin  $S = 10$  and strong anisotropy along the crystallographic  $c$  axis. Application of a magnetic field  $B_{\perp}$  perpendicular to  $c$  induces quantum tunneling between opposite spin orientations, enabling the spins to attain thermal equilibrium. Below  $\sim 0.9$  K, intermolecular interactions turn this equilibrium state into a ferromagnetically ordered phase. However, long range ferromagnetic correlations nearly disappear for  $B_{\perp} \gtrsim 5.5$  T, possibly suggesting the existence of a quantum critical point.

PACS numbers: 75.45.+j, 75.30.Kz, 75.50.Xx

Magnetic nanostructured materials have opened new frontiers for basic science and applications, due to their unique size-dependent properties and the emergence of quantum phenomena [1]. Several fundamental problems remain, however, to be understood. Of particular interest are the observation of phase transitions induced by mutual interactions between nanoscopic magnets in dense arrays. A crucial question here is the mechanism by which the ordered equilibrium phase is attained. For very small magnetic clusters, zero-point quantum fluctuations (e.g. quantum tunneling) are expected to dominate the relaxation process at very low temperatures [2]. Eventually, these fluctuations might even suppress long-range order provided they become sufficiently strong against both interparticle interactions and decoherence [3]. Such a quantum critical point has been observed for 3-D model Ising ferromagnets [4] but its existence for arrays of nanomagnets remains uncertain. Understanding the interplay between ordering and quantum fluctuations can be important for applications of these nanomagnets in ultrahigh density magnetic recording and quantum computation, when it is necessary to control the quantum behavior of entangled interacting qubits.

Usually, however, these phenomena are masked by the particle's size distribution and disorder present in even the most homogeneous samples [5]. By contrast, molecular magnetic clusters [6, 7] are ideal candidates for these studies [8, 9]. In the case of Mn<sub>12</sub> acetate [10], the first and most extensively studied member of the family of single-molecule magnets, clusters contain 12 manganese atoms linked via oxygen atoms, with a sharply-defined and *monodisperse* size. At low temperatures, each of them exhibits the typical behavior of a magnetic nanoparticle, such as slow magnetic relaxation and magnetization hysteresis loops, due to the combination of an  $S = 10$  magnetic ground state with appreciable magnetic anisotropy. And finally, they organize to form tetragonal molecular *crystals*. Since molecular spins couple via dipolar interactions, these crystals are nearly perfect re-

alizations, with magnetic units of mesoscopic size, of the Ising quantum model.

Long-range magnetic order has however not been observed for Mn<sub>12</sub> yet. The reason is that the spin reversal via resonant quantum tunneling [11, 12, 13, 14] becomes extremely slow at low temperatures (of order two months at  $T = 2$  K). For the time scales  $\tau_e \sim 10^2 - 10^4$  s of a typical experiment, the spins are unable to attain thermal equilibrium below a blocking temperature  $T_B \sim 3$  K, which is higher than the ordering temperature  $T_c$ . It has also been argued [9] that hyperfine bias caused by randomly frozen Mn nuclear spins might hinder the occurrence of long-range order in Mn<sub>12</sub>. Here we circumvent these experimental problems by the application of a transverse magnetic field  $B_{\perp}$  that promotes quantum tunneling of the molecular spins. We report neutron diffraction data that point to the existence of long-range ferromagnetic order in Mn<sub>12</sub> that can be suppressed by either increasing temperature up to  $T_c \simeq 0.9(1)$  K or magnetic field, above  $\sim 5.5(5)$  T.

Magnetic diffraction of thermal neutrons is a suitable tool for these studies because neutrons can probe the magnetization along the anisotropy axis [15], i.e. the order parameter, and provide a very accurate determination of the crystal's orientation with respect to the applied magnetic field. The  $\sim 0.5 \times 0.5 \times 1.5$  mm<sup>3</sup> single crystal of deuterated Mn<sub>12</sub> acetate, [Mn<sub>12</sub> (CD<sub>3</sub>COO)<sub>16</sub> (D<sub>2</sub>O)<sub>4</sub>O<sub>12</sub>] · 2 CD<sub>3</sub> COOD · 4D<sub>2</sub>O, was prepared following the original method of Lis [10]. It was glued to a copper rod in good thermal contact with the mixing chamber of a <sup>3</sup>He-<sup>4</sup>He dilution refrigerator, which gives access to the temperature range  $45 \text{ mK} \leq T \leq 4$  K. The  $c$  axis was carefully oriented to be perpendicular to the vertical field  $0 \leq B_{\perp} \leq 6$  T applied by a superconducting magnet. From the orientation matrix measured at zero field and  $T = 4$  K, we estimate that the crystallographic ( $\bar{1}10$ ) direction lay within  $0.1(1)$  degrees of the magnet axis.

At any temperature  $T \leq 4$  K, we measured a series of Bragg diffraction reflections as a function of  $B_{\perp}$  [16].

Each reflection ( $hkl$ ) contains a nuclear  $I_N$  contribution and a magnetic  $I_m$  contribution. The former contains information about atomic order, whereas the latter is proportional to the square of the magnetization components perpendicular to the ( $hkl$ ) direction. The nuclear contribution can be obtained by measuring the intensity at zero field in the paramagnetic phase (see Fig. 1). By subtracting this,  $I_m$  can be estimated at any field and temperature.

Given the strong anisotropy of  $Mn_{12}$ , the magnetization must be confined in the plane defined by the anisotropy axis  $c$  and the magnetic field, with components  $M_z$  and  $M_\perp$  respectively. The experimental protocol followed for each reflection line is illustrated in Fig. 1, where we plot raw rocking curves obtained for the ( $\bar{2}20$ ) reflection. For this example, the momentum transfer is orthogonal to both the magnetic field and the anisotropy axis. In addition, it has a very small nuclear contribution. Therefore the diffracted intensity must be sensitive to both  $M_z$  and  $M_\perp$  components. At 4 K,  $I_m \propto B_\perp^2$ , as expected, since  $M_z = 0$  in the paramagnetic state and  $M_\perp$  is proportional to  $B_\perp$ . At 100 mK, by contrast, a large additional contribution to  $I_m$  shows up in the low-field region (for  $B_\perp < 5$  T). Since  $M_\perp$  is nearly independent of  $T$  (see the inset of Fig. 2), the additional magnetic diffracted intensity reflects the onset of a non-zero

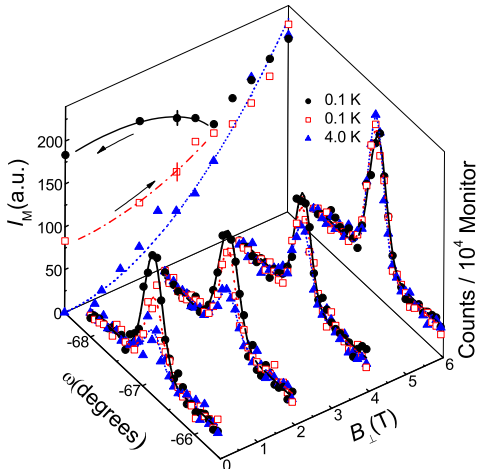


FIG. 1: (Color online) Rocking curves for the ( $\bar{2}20$ ) reflection measured at two different temperatures and four magnetic fields. The counting statistics are typical for such a small crystal under these conditions. The lines are Gaussian fits. Numerical integration of these rocking curves gives the diffracted intensity  $I$ . The magnetic diffraction intensities  $I_m$  were obtained at each temperature and field by subtracting from the total intensity the value measured at 4 K and  $B_\perp = 0$ .  $\Delta$ ,  $T = 4$  K;  $\bullet$  and  $\circ$ ,  $T = 100$  mK measured while increasing and then decreasing  $B_\perp$ , respectively. The dotted line is a least squares fit to a parabola  $AB_\perp^2$ .

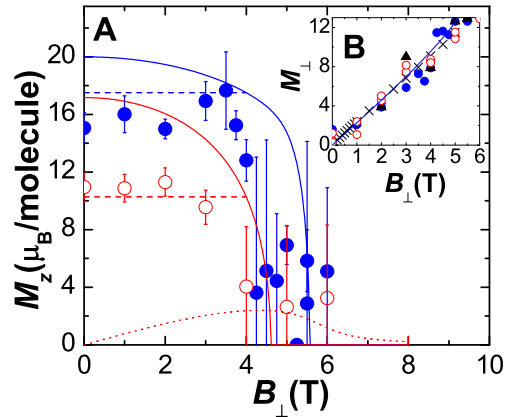


FIG. 2: (Color online) **A** Longitudinal magnetization  $M_z$  of  $Mn_{12}$  acetate measured while decreasing the transverse magnetic field from 6 T.  $\bullet$  and  $\circ$  are for  $T = 47$  mK and 600 mK, respectively. Solid lines are calculated using Eq. (1) and the parameters given in the text. Horizontal dashed lines show  $M_z$  calculated at 4 T, below which spins are 'frozen' by the anisotropy energy barriers. The dotted line shows  $M_z$  induced at  $T = 600$  mK by the small misalignment of the crystal in the case of no interactions ( $J_{\text{eff}} = 0$  in Eq. (1)). **B**  $\times$  perpendicular magnetization  $M_\perp$  obtained at  $T = 4$  K with a SQUID magnetometer. Data obtained from neutron diffraction are also shown:  $\bullet$ ,  $T = 47$  mK;  $\circ$ ,  $T = 600$  mK;  $\blacktriangle$ ,  $T = 4$  K.

$M_z$ . Furthermore, this low- $T$  contribution shows hysteresis. Indeed, as shown in Fig. 1,  $I_m$  data measured while *increasing*  $B_\perp$  after the sample was cooled at zero field from  $T \simeq 1$  K, lie clearly below those measured while *decreasing* it, merging approximately at  $B_\perp = 4(1)$  T. The hysteresis means that spins can attain equilibrium within the experimental time  $\tau_e \simeq 7 \times 10^3$  s only above  $B_\perp = 4$  T. The fact that this field-induced "jump to equilibrium" happens at approximately the same field for  $T = 100$  mK and  $T = 600$  mK confirms that relaxation to equilibrium proceeds via temperature-independent tunneling processes [17, 18].

To obtain  $M_z$  and  $M_\perp$  as a function of magnetic field (Fig. 2) and temperature (Fig. 3), several reflection lines were simultaneously fitted and the results calibrated against SQUID magnetization measurements performed at 4 K. At our minimum temperature  $T = 47$  mK,  $M_z$  is approximately zero for  $B_\perp \gtrsim 5.5(5)$  T and then it increases when decreasing  $B_\perp$ , reaching  $16\mu_B$  per molecule at zero field. The temperature dependence of this zero-field  $M_z$  is shown in Fig. 3. It is approximately constant until it begins decreasing sharply for  $T \gtrsim 0.6$  K. Above 1 K, as at 4 K, the fit gives  $M_z \sim 0$ .

These experiments show without ambiguity the existence of a net magnetization along the anisotropy axis and that it vanishes at sufficiently high temperatures and

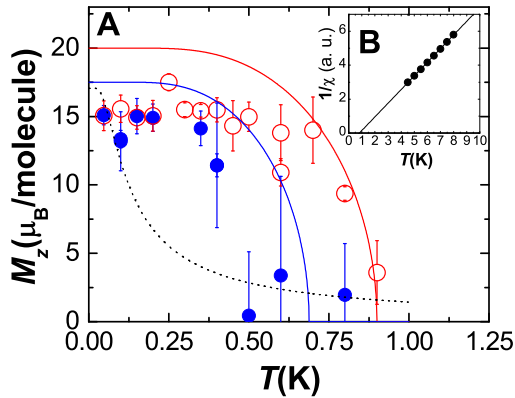


FIG. 3: (Color online) (A) Longitudinal magnetization  $M_z$  obtained from neutron diffraction data measured at  $B_{\perp} = 0$  ( $\circ$ ) and 4 T ( $\bullet$ ). Measurements were recorded after cooling the sample in zero field and subsequently applying  $B_{\perp} = 6$  T before setting the final field. The dotted line shows  $M_z$  arising from the maximum misalignment (0.1 deg.) of the crystal at  $B_{\perp} = 4$  T. Solid lines are calculations (for perfect orientation) that include interactions via the mean-field Hamiltonian (1). (B) Reciprocal equilibrium susceptibility measured at  $T > 4.5$  K along the  $c$  axis. The line is a least-squares linear fit, giving  $T_c = 0.8(1)$  K.

perpendicular magnetic fields. The qualitative resemblance between  $M_z$  vs  $B_{\perp}$  and  $M_z$  vs  $T$  curves is typical of quantum ferromagnetic systems [4]. However, for such a strong anisotropy, any deviation of the crystal from the perpendicular orientation can induce, at  $B_{\perp} > 4$  T, some magnetic polarization along the anisotropy axis [18] that would then remain frozen below the irreversibility field (4 T). In our case, this deviation is known from "high"-temperature diffraction data to be smaller than 0.1 degrees, which agrees fully with the small  $M_z$  values measured at  $B_{\perp} = 4$  T and above 500 mK. In Figs. 2 and 3 we show that such a small misalignment cannot account, by itself, for  $M_z$  observed at  $T > 100$  mK. In addition, for  $T > 400$  mK,  $M_z$  increases significantly as the field is reduced to zero from  $B_{\perp} = 4$  T, showing that, even at zero field, the spins tend to polarize as they approach equilibrium. The existence of long-range magnetic order is also supported by the finite temperature intercept (0.8(1) K) of the reciprocal paramagnetic susceptibility shown in the inset of Fig. 3. We therefore conclude that  $\text{Mn}_{12}$  acetate is a ferromagnet for  $T < T_c \sim 0.9(1)$  K and  $B_{\perp} < B_c \sim 5.5(5)$  T. The ferromagnetic nature of the ordered phase agrees with theoretical predictions [8], which however predict  $T_c \sim 0.45$  K, lower than observed. In our view, the discrepancy might arise from the fact that Monte Carlo calculations were performed for point-like spins, whereas  $\text{Mn}_{12}$  molecules are extended nanoscopic objects [19]. It is worth mentioning that the relatively

strong hyperfine interactions do not prevent the ordering of  $\text{Mn}_{12}$  molecular spins probably because, as has been observed recently [2, 17], Mn nuclear spins also fluctuate rapidly when tunneling rates are sufficiently fast.

These qualitative interpretation can be put on a solid basis with the help of theoretical calculations. A simple way to introduce interactions in the analysis is by making use of a mean-field approximation

$$\mathcal{H} = -DS_z^2 + C(S_+^4 + S_-^4) - g\mu_B (B_x S_x + B_y S_y) - J_{\text{eff}} \langle S_z \rangle S_z \quad (1)$$

where  $D$  and  $C$  are the uniaxial and in-plane anisotropy constants,  $g = 2$  the gyromagnetic ratio,  $B_x$  and  $B_y$  are the magnetic field components along  $a$  and  $b$ ,  $J_{\text{eff}}$  is a mean-field interaction parameter, and  $\langle S_z \rangle = M_z/g\mu_B$  is the thermal statistic average of  $S_z$ . We estimated  $D = 0.62k_B$  by fitting the perpendicular magnetization measured at 4 K, while  $C$  has been set to  $2.5 \times 10^{-4}$  K in order to fit the critical field  $B_c = 5.5$  T. These are of the same order as the values obtained by spectroscopic techniques [20]. We also set  $J_{\text{eff}} \simeq 4.5 \times 10^{-3}k_B$  to account for the experimental  $T_c \simeq 0.9$  K.

We have calculated  $M_z$  and  $M_{\perp}$  by performing a numerical diagonalization of Eq.(1) followed by a self-consistent calculation of the statistically averaged spin components. Field- and temperature-dependent calculations account reasonably well for  $M_z$  and  $M_{\perp}$ , predicting in particular the vanishing of  $M_z$  at either  $B_c$  or  $T_c$ . The incomplete saturation of  $M_z$  at zero field arises probably from 'down' spins that remain frozen below  $B_{\perp} = 4$  T because the quantum tunneling rates become too slow at such low fields. We face here the curious situation that quantum fluctuations, which can eventually suppress magnetic order, are nevertheless necessary to attain equilibrium. In Figure 4, we show the magnetic phase diagram of  $\text{Mn}_{12}$  acetate obtained from our experiments. Application of a perpendicular field tends to shift  $T_c$  significantly towards lower temperatures. As before, the mean-field calculations reproduce reasonably well the overall features.

Summing up, our experiments on  $\text{Mn}_{12}$  nanomagnets show the existence of a ferromagnetic phase below  $T_c \simeq 0.9$  K that can be suppressed by the application of an external magnetic field. Deciding if this field-induced transition is driven purely by quantum fluctuations requires measuring the critical behavior of  $M_z$  [3], which is clearly beyond the sensitivity of the present experiments. What we do observe is that, above  $B_c \sim 5.5$  T, the order parameter  $M_z$  vanishes even at the lowest accessible temperatures ( $T > 47$  mK in our case). We note that  $B_c$  is about two thirds of the anisotropy field  $2SD/g\mu_B \sim 9$  T that would be required to saturate the  $\text{Mn}_{12}$  spins along a hard axis if they were *classical* spins. In fact, as shown in the inset of Fig. 2,  $M_{\perp}$  is still much smaller than saturation at  $B_c$ . These facts and the agreement with mean-field calculations make it plausible that quantum

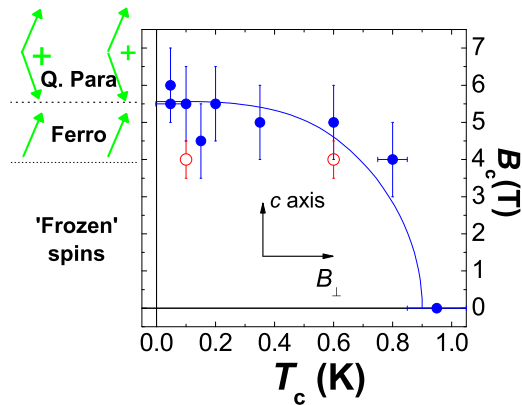


FIG. 4: (Color online) Magnetic phase diagram of Mn<sub>12</sub> acetate. The solid dots show the critical magnetic field  $B_c$  at which the longitudinal magnetization is observed to vanish at each temperature. The open dots give the irreversibility field, below which spins do not attain equilibrium within the experimental time. The solid line was obtained from magnetization curves calculated in a mean-field approximation (Eq. (1)).

fluctuations can suppress long-range order. Within this interpretation,  $M_z$  vanishes because the quantum tunnel splitting  $\Delta$  induced by off-diagonal terms of Eq. (1) dominates over dipolar interactions. Therefore, at  $T = 47$  mK almost all molecular spins should be in their ground state, which becomes a superposition of 'spin-up' and 'spin-down' states, a mesoscopic magnetic "Schrödinger's cat" [21]. Previously, the existence of quantum superpositions of spin states was derived from the detection of  $\Delta$  [17, 22, 23], while here we have monitored the vanishing of the  $z$  spin component.

Similar collective magnetic phenomena could be observed in arrays of larger nanomagnets, like magnetic nanoparticles, provided they are sufficiently ordered and monodisperse, requirements that appear to be within the reach of modern synthetic procedures [5]. The existence of "super-ferromagnetism" was predicted more than ten years ago [24]. However, besides indications of the collective, spin-glass-like, nature of the magnetic relaxation [25], no clear-cut experimental evidence for long-range order has been found yet. The present and some other recent results [2] show that bottom-up synthesis can provide physical realizations of these super-ferromagnets albeit on a smaller size scale. Furthermore, quantum dynamics can be used to overcome the slow relaxation and to switch between the ordered and paramagnetic phases.

The authors are grateful to J. L. Ragazzoni and D. Culebras for technical assistance. We acknowledge useful comments on this work by J. F. Fernández. This work is part of the research project MAT02-433 funded by Spanish MCyT. It was partly supported by the European Commission under project IST-NANOMAGIQC.

The authors acknowledge financial support of the ILL for the preparation of the samples.

- 
- [1] E. M. Chudnovsky and J. Tejada, *Macroscopic Quantum Tunneling of the Magnetic Moment*, Cambridge University Press (Cambridge, 1998).
  - [2] M. Evangelisti et al., Phys. Rev. Lett. **93**, 117202 (2004).
  - [3] S. L. Sondhi, S. M. Girvin, J. P. Carini, and D. Sahar, Rev. Mod. Phys. **69**, 315 (1997).
  - [4] D. Bitko, T. F. Rosenbaum, and G. Aeppli, Phys. Rev. Lett. **77**, 940 (1996).
  - [5] S. Sun, C. B. Murray, D. Weller, L. Folks, and A. Moser, Science **287**, 1989 (2000).
  - [6] G. Christou, D. Gatteschi, D. N. Hendrickson, and R. Sessoli, MRS Bull. **25**, 56 (2000).
  - [7] D. Gatteschi and R. Sessoli, Angew. Chem. Int. Ed. **42**, 268, (2003).
  - [8] J. F. Fernández and J. J. Alonso, Phys. Rev. B **62**, 53 (2000).
  - [9] X. Martinez-Hidalgo, E.M. Chudnovsky, and A. Aharony, Europhys. Lett. **55**, 273 (2001).
  - [10] T. Lis, Acta Crystallogr. B **36**, 2042 (1980).
  - [11] J. R. Friedman, M. P. Sarachik, J. Tejada, and R. Ziolo, Phys. Rev. Lett. **76**, 3830 (1996).
  - [12] J. M. Hernández, et al., Europhys. Lett. **35**, 301 (1996).
  - [13] L. Thomas, et al., Nature **383**, 145 (1996).
  - [14] L. Thomas, A. Caneschi, and B. Barbara, Phys. Rev. Lett. **83**, 2398 (1999).
  - [15] Robinson et al., J. Phys. Condens. Mater **12**, 2805 (2000).
  - [16] Neutron diffraction experiments were carried out on the diffractometer D10 at the Institut Laue Langevin. We worked in a two-axis normal-beam configuration at a neutron wavelength of 2.36 Å.
  - [17] F. Luis, F. L. Mettes, J. Tejada, D. Gatteschi, and L. J. de Jongh, Phys. Rev. Lett. **85**, 4377 (2000).
  - [18] I. Chiorescu, R. Giraud, A. Jansen, A. Caneschi, and B. Barbara, Phys. Rev. Lett. **85**, 4807 (2000).
  - [19] Approximating Mn<sub>12</sub> by point-like spins gives interaction energies within 2 % of the exact result only when the intermolecular distances exceed 5 lattice parameters. For shorter distances, the disk-like shape of the Mn<sub>12</sub> molecule reinforces dipolar interactions along the  $a$  or  $b$  axes with respect to interactions along  $c$ . Following simple arguments [8], this should lead to an enhancement of  $T_c$ . The size and shape of the nanostructure becomes an additional factor to determine (and eventually tailor) the physical behavior of the array.
  - [20] A. L. Barra, D. Gatteschi, and R. Sessoli, Phys. Rev. B **56** 8192 (1997).
  - [21] E. Schrödinger, Naturwissenschaften **23**, 807 (1935). English translation in *Quantum Mechanics and Measurement*, edited by Wheeler and Zurek, Princeton University Press (Princeton, 1981).
  - [22] E. Del Barco, et al., Europhys. Lett. **47**, 722 (1999).
  - [23] G. Bellessa, N. Vernier, B. Barbara, and D. Gatteschi, Phys. Rev. Lett. **83**, 416 (1999).
  - [24] S. Mørup, Hyp. Interact. **90**, 171 (1994).
  - [25] T. Jonsson et al., Phys. Rev. Lett. **75**, 4138 (1995).